# EPR study of electron traps in x-ray-irradiated yttria-stabilized zirconia

C. B. Azzoni and A. Paleari

*Dipartimento di Fisica, Alessandro Volta dell'Università di Pavia, via Bassi 6, 27100 Pavia, Italy*

Single crystals of yttria-stabilized zirconia (12 mol % of $Y_2O_3$) have been x-ray irradiated at room temperature. The electron paramagnetic resonance spectrum of the filled electron traps is analyzed in terms of a single oxygen vacancy type of defect with its symmetry axis along the $\langle 111 \rangle$ direction. The angular dependence of the linewidth and the asymmetry of the line shape are attributed to the disordered rearrangements of the anion sublattice surrounding the oxygen vacancy. This affects the local crystal fields and the directions of the symmetry axis of the defects.

## I. INTRODUCTION

The cubic fluorite phase is stabilized in $ZrO_2$ down to room temperature by the presence of trivalent yttrium ions in cation sites. The addition of substitutional heterovalent ions produces a large concentration of oxygen vacancies that is responsible for the ionic conductivity of this material.[1] The study of the structure of these oxygen vacancies and their dependence on the composition and treatment of the material is important for many technological applications (e.g., fuel cells, oxygen sensors, oxygen pumps).

It is known that hydrogen-reducing treatments or current flows or ionizing irradiation fill electron traps connected with the oxygen vacancies. There are many studies of their electrical and optical properties while only a small number of investigations of their structure have been carried out with electron paramagnetic resonance (EPR) spectroscopy.

One of the main features of the oxygen sublattice is the disordered relaxations of the anion positions around the oxygen vacancies, as observed in neutron,[2] electron,[3] and x-ray diffraction[4] studies. Some consequences of this disorder have been observed in optical spectra where the absorption and emission bands of intrinsic defects[5-7] or local microprobes, such as $Er^{3+}$ and $Eu^{3+}$,[8,9] are anomalously broadened. The disordered rearrangement of the oxygens around the vacancies creates crystal fields at the cation positions, slightly different from site to site, and results in inhomogeneous broadening of the spectral bands. Evidence of these features have not been reported from EPR until now.

In this paper we present the results of EPR measurements performed on oriented single crystals of x-ray irradiated yttria-stabilized zirconia (YSZ). The data are analyzed in terms of a single paramagnetic defect with local axial symmetry in four equally probable orientations with respect to the crystal axis, as already proposed.[10-12] The refinement of the experimental conditions allowed us to detect some features of the signal that may be interpreted as evidence of small deviations from the previously cited axial $\langle 111 \rangle$ symmetry of the defects, perhaps due to the effect of the disordered rearrangements of the oxygens. On the basis of these data and also to explain the angular

dependence of the linewidth, we propose a model of electron trapping near an oxygen vacancy somewhat different from an $F$ center, that is the attribution suggested up to now.

## II. EXPERIMENTAL DETAILS

Single crystals of $ZrO_2-12$ mol % $Y_2O_3$ from Ceres Corporation were oriented and cut along $\langle 100 \rangle$ directions with the aid of an x-ray diffractometer. One of the as-received crystals was taken as a reference sample while another was x-ray irradiated at room temperature (120 sec, W target, 20 mA, 38 kV). The perfectly transparent appearance of the as-received crystals changed to a slightly smoky coloration after irradiation. The sample, whose dimensions are $1 \times 1 \times 8$ mm$^3$, was mounted on a goniometer by using two types of sample holder that allowed the direction of the rotation axis to be fixed parallel to a $\langle 100 \rangle$ direction or orthogonal to a $\langle 111 \rangle$ direction. In Fig. 1 the relations between crystal axis, rotation axis, and magnetic-field direction are shown for the two experimental configurations. EPR measurements ($X$-band) were performed at 150 K and room temperature. No differences were found except for a decreasing area
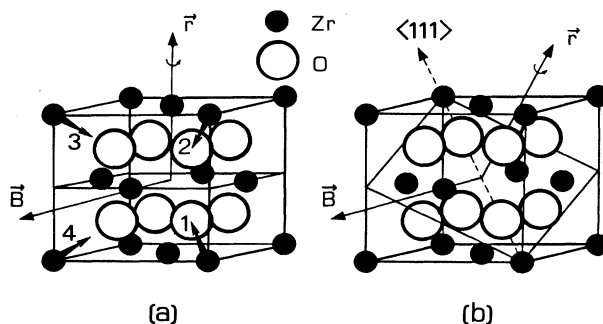


FIG. 1. Unit cell of YSZ together with the magnetic-field direction and the axis around which the crystal is rotated for the two adopted experimental configurations. In (a) the four possible orientations of the defect axis are indicated by the numbered arrows.

with increasing temperature, according to the Boltzmann factor. Different microwave powers, up to about 300 mW, were employed to verify the absence of saturation effects. The modulation intensity was kept at suitably low values $(3 \times 10^{-2}$ mT in the narrower-linewidth condition).

## III. RESULTS

The as-received crystals do not exhibit any EPR signal, contrary to that observed in an early work[10] and probably due to accidental impurities present in the samples.

The EPR spectrum of the irradiated crystal consists of two signals when the magnetic field direction varies in a $\{100\}$ crystalline plane, while it is composed of four signals when the magnetic field is rotated in a $\{221\}$ plane. The observed angular variation of the spectra is what one should expect in the case of paramagnetic defects with their axis of symmetry along any of the four $\langle 111 \rangle$ directions, with $g_\parallel = 1.989$ and $g_\perp = 1.852$ as principal values of the g tensor. The calculated curves (see Fig. 2) reproduce the angular behavior of the EPR lines within the experimental error (the crystal orientation is accurate within a few degrees). It should be noted that curve 2 in Fig. 2(b) is always superimposed on the other lines resulting in a

distorted signal. Also, the ratios between the signal areas correspond to a fourfold multiplicity of defects, a single line being due to about a fourth of the total spin concentration, estimated to be $10^{17}$ cm$^{-3}$ from a comparison with the Varian standard pitch sample.

The observed spectra have a variable linewidth, whose angular dependence has a $\pi$ periodicity. The maximum width is detected when the magnetic field is directed orthogonally to the $\langle 111 \rangle$ axis, resulting in Gaussian symmetric lines about 6 mT in width $(\Delta B_\perp)$. Decreasing the angle between $B$ and a $\langle 111 \rangle$ direction, the line shape becomes more and more asymmetric. This is particularly evident when the magnetic field lies in a $\langle 111 \rangle$ direction and the EPR signal reaches a minimum of 0.7 mT for the linewidth $(\Delta B_\parallel)$. Generally, an asymmetry of the EPR signal is associated with an angular distribution of anisotropic paramagnetic centers that, in the case of completely random orientations, gives rise to powder patterns. We tried to simulate the experimental asymmetry allowing an angular distribution of the directions of the defect axis, limited to a few degrees around the $\langle 111 \rangle$ directions. The good fit (see Fig. 3) indicates a detectable deviation of the symmetry axis of the defects from the $\langle 111 \rangle$ directions, with a distribution of angles between 0° and $4° \pm 2°$, the uncertainty deriving from the limits in the accuracy of the crystal orientation. The line shape is intermediate between a pure Lorentzian function and a pure Gaussian. No hyperfine structure (HFS) has been detected.

## IV. DISCUSSION

### A. Anisotropy of the g tensor

The axiality of the defect is accounted for by supposing that the EPR center experiences an axial crystal field. Two cases may occur, both giving the correct angular dependence of the g value but possessing other discriminating features.

(a) The unpaired spin may be in an anion site, at an oxygen vacancy, whose crystal field is given by three zir-
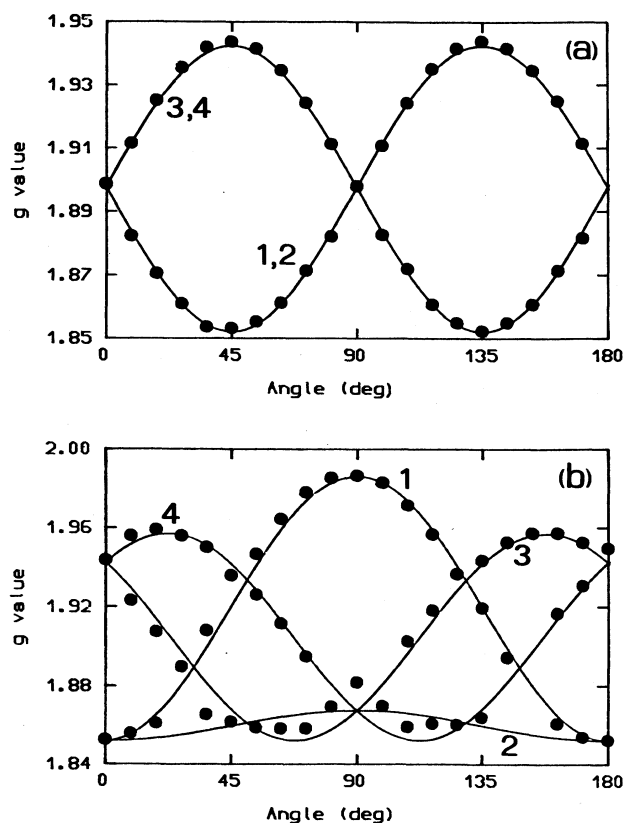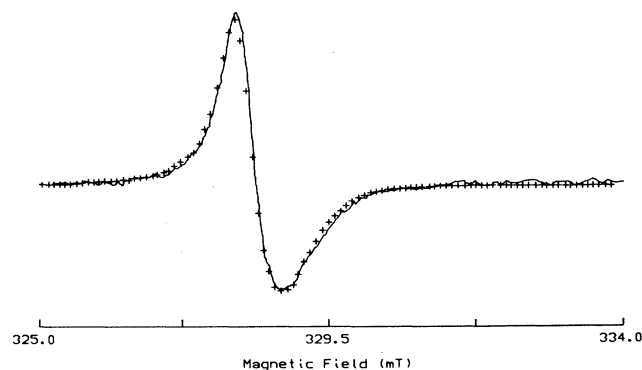


FIG. 2. Angular dependence of the g values of the EPR signals observed in x-ray-irradiated YSZ. The magnetic field lies (a) in a $\{100\}$ plane, (b) in a $\{221\}$ plane. The curves are labeled according to the four possible defect axis orientations indicated in Fig. 1.



FIG. 3. EPR derivative signal of x-ray-irradiated YSZ for $B\|\langle 111 \rangle$ axis. The experimental asymmetric line shape (solid line) is simulated (crosses) under the assumption of small deviations $(\theta \leq 8°)$ of the defect axis from the $\langle 111 \rangle$ crystal directions and a spread of the $g_\perp$ value (see text).

conium ions and one yttrium ion. The electronic wave function of such an $F^+$ center should be a linear combination of the atomic orbitals of the surrounding cations[13] (primarily $4p$, $4d$, and $5s$ wave functions of Zr and Y atoms).

(b) The cation site near an anion vacancy may constitute an electron trap subjected to the crystal field of seven coordinated oxygens. The unpaired spin would be a $4d$ electron of a $Zr^{3+}$ in a distorted cubic electric potential.

From the first model, the only one proposed up to now, one derives two strong conditions to the distribution of the defects in YSZ: (i) one-to-one correlation between oxygen vacancies and yttrium ions; (ii) oxygen vacancies as nearest neighbors of the trivalent cations. If one or both of these conditions are not strictly met, one should observe an isotropic EPR signal from that percentage of electrons that are trapped in the tetrahedrally symmetric environments of four zirconium ions. Actually, points (i) and (ii) are matters of discussion and precise answers are not yet available.[9,14−18]

It should be noted that no hyperfine structure has been detected from $^{91}$Zr or from $^{89}$Y. However, in the first case (12 at. % abundant $^{91}$Zr with $I = \frac{5}{2}$), the hyperfine lines would hardly be observable, their intensity being about 70 times smaller than the central line of the zero nuclear-spin isotope. But in the case of interaction between the spin of the $F^+$ center and the necessarily associated yttrium nuclei, one should observe the EPR signal split into a doublet, the nuclear spin of the 100% abundant $^{89}$Y isotope being $I = \frac{1}{2}$.

The second model does not imply the presence of a trivalent cation near the trapped electron: The anisotropy and the axiality of the $g$ value along the $\langle 111 \rangle$ directions are provided by the axial component of crystal field arising from the presence of an oxygen vacancy near the eptacoordinated zirconium in a $4d^1$ electronic configuration. The cubic component of the field splits the orbital degeneracy, lowering the energy of the $\Gamma_3$ doublet with respect to the $\Gamma_5$ triplet. The displacements of the anions surrounding the oxygen vacancy decrease the Zr-O distances (about 10%) and create an axial distortion of the cubic field that forces the $|3z^2 - r^2\rangle$ state at the ground level. In this case the principal values of the $g$ tensor are[19]

$$g_\| = 2[1 + (\tfrac{3}{2})(\lambda/\Delta)^2]^{-1} ,$$
$$g_\perp = [2 - 6(\lambda/\Delta)][1 + (\tfrac{3}{2})(\lambda/\Delta)^2]^{-1} , \quad (1)$$

where $\lambda$ is the spin-orbit coupling constant [about 500 cm$^{-1}$ for $Zr^{3+}$ (Ref. 19)] and $\Delta$ is the crystal-field energy splitting. It may be noted that the relations (1) give $g_\| > g_\perp$ where $g_\|$ depends on $\lambda/\Delta$ only to second order, while $g_\perp$ has a first-order dependence, so that $g_\| \lesssim 2$, $g_\perp \simeq 2 - 6(\lambda/\Delta)$, and $\Delta \simeq 2 \times 10^4$ cm$^{-1}$.

## B. Anisotropy of the linewidth

The strong angular dependence of the linewidth has just been observed by other authors,[10−12] but never explained. Generally, such a dependence is expected when there are directional interactions such as hyperfine or dipolar spin-spin interactions. Hyperfine interaction in the directions between anions and cations is in contradiction with the observed minimum of broadening and absence of HFS when the magnetic field is oriented along a $\langle 111 \rangle$ axis. Dipolar interactions are not likely to be responsible for the effect because of the low concentration of paramagnetic defects (i.e., about $10^{17}$ cm$^{-3}$) while the experimental broadening of a few mT should involve a higher density of EPR centers with a maximum distance between them of about twice the lattice parameter ($a_0 \cong 0.515$ nm). Also, the presence of defect clusters, locally possessing a high density of EPR centers, would not explain the experimental angular dependence of broadening that is not compatible with the typical $3\cos^2\theta - 1$ law of these interactions.

On the contrary, taking into account the existence of distortions in the anion lattice around the oxygen vacancy, detected by many authors by using other techniques,[2−7] the second model proposed in the preceding section, involving an oxygen vacancy near a $Zr^{3+}$ may suggest a possible explanation of the angular dependence of the linewidth. In fact, the different dependence of the principal values of the $g$ tensor on the parameter $\Delta$ [see Eq. (1)] results in a $g_\|$ value nearly unaffected by variations of the crystal-field parameter induced by the different anion environments. In contrast, the $g_\perp$ value is almost linearly dependent on $\lambda/\Delta$. Then, if there is a sufficient spread in the crystal-field values, this will imply $\Delta B_\perp \gg \Delta B_\|$ and, as a consequence, the linewidth will depend on the spread in the $g_\perp$ value:

$$\Delta B_\perp = (B_\perp/g_\perp)|\Delta g_\perp| \quad \text{where} \quad \Delta g_\perp = 2.84 \times 10^{-2} . \quad (2)$$

From this relation the spread of the crystal-field parameter $\Delta$ may be evaluated:

$$\Delta \cong 6\lambda/[2 - (g_\perp \pm \Delta g_\perp/2)] \quad \text{from which} \quad \delta\Delta/\Delta \cong 20\% . \quad (3)$$

One finds that the observed magnitude of the anion dislocation (about 0.02 nm along the $\langle 100 \rangle$ directions) is compatible with the supposed spread of $\Delta$. Remembering that the predominant cubic field parameter is inversely proportional to the fifth power of the cation-anion distance,[19] we obtain

$$\delta\Delta/\Delta \cong \langle R \rangle^5 (R'^{-5} - R^{-5}) \quad \text{yielding} \quad \delta\Delta/\Delta \cong 25\% , \quad (4)$$

where $R$ and $R'$ are the maximum (about 0.223 nm) and the minimum (about 0.210 nm) of the Zr-O distance[2] in YSZ, respectively.

An expression for the linewidth versus $\theta$ may be obtained from the condition of resonance and the angular dependence of $g$:

$$\Delta B(\theta) = (g_\perp^2 \Delta B_\perp/B_\perp)[B(\theta)/g^2(\theta)]\sin^2\theta , \quad (5)$$

where $\theta$ is the angle between the direction of the magnetic field and $\langle 111 \rangle$ axis. In Fig. 4 the calculated curve (curve 1) together with the experimental linewidths are shown: There is a good agreement except for some
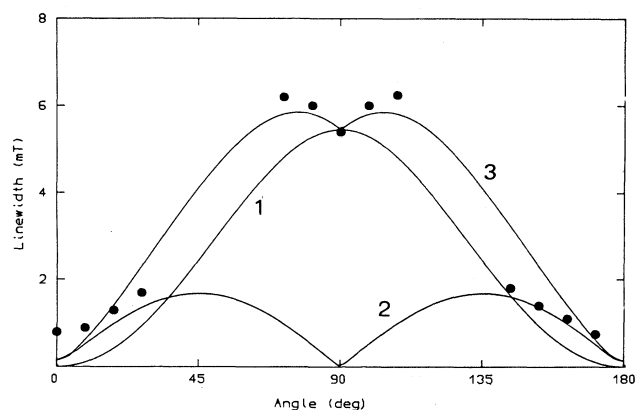
FIG. 4. Experimental linewidths of the EPR signal vs the angle between $B$ and a $\langle 111 \rangle$ axis. The plot of Eq. (5) is also shown (curve 1) together with the curve that takes into account the effect of the angular distribution of the defect axis discussed in the text (curve 2). The curve 3 is the sum of the two contributions.

features around 90° and the absence of data around 45° (owing to the superposition of signals from different sites). In the next paragraph, experimental evidence is presented that may explain these features.

### C. Asymmetry of the line shape

The disordered distribution of the rearrangements of the oxygen positions around the anion vacancies causes not only a variation of the electric potential at the cation sites, but also, in general, a change of the direction of the symmetry axis of the defects. The powderlike feature of the signals, and particularly of the narrow signal that we have analyzed for $B$ nearly parallel to a $\langle 111 \rangle$ direction, may constitute evidence of this fact and represents the first direct EPR observation of the "glasslike" nature of the oxygen sublattice in YSZ. It may be noted that the simulated distribution of the angle between the defect axis and the $\langle 111 \rangle$ direction of the crystal is the right order of magnitude expected from the ionic displacements in the cubes of oxygens: The angle formed by the two

vectors $\underline{R}$ and $\underline{R}'$ connecting the cation and the anion in the condition of maximum and minimum of the Zr-O distance is about 4°.

The effects of the deviations of the symmetry axis of the defects from the $\langle 111 \rangle$ directions should contribute to the line broadening for all the orientations of the magnetic field with respect to the crystal axis. The angular dependence of this source of broadening, following a $\sin 2\theta$-like law, is shown in curve 2 of Fig. 4 where the angle between the $\langle 111 \rangle$ directions and the defect axis varies from $-2°$ to $+2°$. It may be noted that the behavior of the linewidth around 90° is qualitatively accounted for by this dependence [in curve 3 of Fig. 4 this effect is added to the broadening predicted by Eq. (5)].

### V. CONCLUSION

The EPR signal of the paramagnetic axial defects activated in YSZ after x-ray irradiation have been studied by considering (i) the anisotropy of the spectra; (ii) the $g$ values with $g_{\parallel} > g_{\perp}$; (iii) the absence of hyperfine structure from $^{89}$Y; (iv) the linewidth behavior related to inhomogeneous broadening (deriving from a spread of only the $g_{\perp}$ value) rather than to directional interactions; and (v) the asymmetry of the signal, particularly evident in the condition of minimum broadening.

As a result we propose a model that fits many experimental features. It invokes a trapped electron in a $4d^1$ configuration of the eptacoordinated zirconium ions near the oxygen vacancies. Surely this assignment needs additional experimental verifications, but it is surprisingly compatible with the peculiar behavior of the oxygen sublattice previously never probed by EPR spectroscopy.

[1]E. C. Subbarao and H. S. Maiti, Solid State Ionics **11**, 317 (1984).

[2]D. Steele and B. E. F. Fender, J. Phys. C **7**, 1 (1974).

[3]S. Suzuki, M. Tanaka, and M. Ishigame, J. Phys. C **20**, 2963 (1987).

[4]J. B. Cohen, M. Morinaga, and J. Faber, Jr., Solid State Ionics **3/4**, 61 (1981).

[5]K. A. Shoaib, F. H. Hashmi, M. Ali, S. J. H. Bukhari, and C. A. Majid, Phys. Status Solidi A **40**, 605 (1977).

[6]P. A. Arsenev, K. S. Bagdasarov, A. Niklas, and A. D. Ryazantsev, Phys. Status Solidi A **62**, 395 (1980).

[7]M. Kunz, H. Kretschmann, W. Assmus, and C. Klingshirn, J. Lumin. **37**, 123 (1987).

[8]H. Arashi, Phys. Status Solidi A **10**, 107 (1972).

[9]J. Dexpert-Ghys, M. Faucher, and P. Caro, J. Solid State Chem. **54**, 179 (1984).

[10]J. S. Thorp, A. Aypar, and J. S. Ross, J. Mater. Sci. **7**, 729 (1972).

[11]J. Shinar, D. S. Tannhauser, and B. L. Silver, Solid State Commun. **56**, 221 (1985).

[12]J. Shinar, D. S. Tannhauser, and B. L. Silver, Solid State Ionics **18 & 19**, 912 (1986).

[13]S. A. Al'tshuler and B. M. Kozyrev, *Electron Paramagnetic Resonance* (Academic, New York, 1964).

[14]M. Morinaga, J. B. Cohen, and J. Faber, Jr., Acta Crystallogr. **36**, 520 (1980).

[15]C. R. A. Catlow, A. V. Chadwick, G. N. Greaves, and L. M. Moroney, J. Am. Ceram. Soc. **69**, 272 (1986).

[16]M. H. Tuillier, J. Dexpert-Ghys, H. Dexpert, and P. Lagarde, J. Solid State Chem. (to be published).

[17]S. Badwal, J. Mater. Sci. **19**, 1767 (1984).

[18]T. Uehara, K. Koto, S. Emura, and F. Kanamaru, Solid State Ionics **23**, 331 (1987).

[19]A. Abragam and B. Bleaney, *Electron Paramagnetic Resonance of Transition Ions* (Oxford University Press, New York, 1970).